JVI Journals.ASM.org

Formation of Higher-Order Foot-and-Mouth Disease Virus 3D^{pol} Complexes Is Dependent on Elongation Activity

Matthew Bentham, Kris Holmes, Sophie Forrest, David J. Rowlands, and Nicola J. Stonehouse

Institute of Molecular and Cellular Biology, Faculty of Biological Sciences and Astbury Centre for Structural Molecular Biology, University of Leeds, Leeds, United Kingdom

The replication of many viruses involves the formation of higher-order structures or replication "factories." We show that the key replication enzyme of foot-and-mouth disease virus (FMDV), the RNA-dependent RNA polymerase, forms fibrils *in vitro*. Although there are similarities with previously characterized poliovirus polymerase fibrils, FMDV fibrils are narrower, are composed of both protein and RNA, and, importantly, are seen only when all components of an elongation assay are present. Furthermore, an inhibitory RNA aptamer prevents fibril formation.

Foot-and-mouth disease virus (FMDV) is one of the most important animal pathogens of agricultural significance, yet key aspects of its replication are still unclear. The virus occurs as seven distinct serotypes and is a member of the *Picornaviridae*, which also includes important human pathogens, such as poliovirus (PV) and rhinovirus. Replication of the positive-stranded RNA genome occurs via a negative-stranded intermediate and involves several viral proteins as well as specific sequences within the untranslated regions (UTRs) at the 5′ and 3′ ends. The 5′ UTR is exceptionally long (~1,200 nucleotides), constituting one-seventh of the viral genome. It includes a 400-nucleotide region predicted to be double stranded in structure (3), a poly(C) tract of ~200 nucleotides (20), a series of pseudoknots (3, 6), a *cis*-acting replication element (cre) necessary for the uridylation of the peptide primer of replication (VPg) (13, 15), and an internal ribosome entry site (IRES) necessary for the initiation of protein synthesis (18). The 3′ UTR is shorter but includes two stem-loop structures and a poly(A) tract. Several of these RNA structural elements are known or thought to be important in genome replication. The engine of genome replication is an RNA-dependent RNA polymerase enzyme (RdRp), termed 3D^{pol}, with the involvement of its precursor, 3CD. RNA synthesis is primed by a uridylated form of VPg, which is the product of the 3B gene. Uniquely, the FMDV genome encodes three tandem copies of 3B (VPg), and it is tempting to speculate that this feature is causally linked to the exceptionally fast replication rate characteristic of the virus. Some strains of FMDV complete the entire life cycle in only 3 h *in vitro* (20). Uridylation of VPg to form VPgpUpU is carried out by 3D^{pol} but requires the presence of 3CD in an ancillary catalytic role to work efficiently (15). Although synthetic versions of VPg peptide can be uridylated *in vitro*, the true precursor *in vivo* (3AB or 3BCD) is unknown and controversial. Replication of the viral genome is complex and difficult to study *in vivo*, but aspects of the process can be replicated *in vitro*, making them more amenable to investigation.

Replication of many positive-stranded RNA viruses is thought to occur in "factories" (4), allowing compartmentalization, concentration, and protection of the components and products. Consistent with this, FMDV 3D^{pol} has been shown to concentrate on membranes of small, smooth vacuoles (19). The Kirkegaard group has identified fibrous structures (approximately 120 Å in diameter) associated with membranes within PV-infected cells. Furthermore, they have demonstrated that recombinant PV 3D^{pol} alone can form fibers/fibrils, sheets, and tubes of 400 to 1,000 Å in diameter *in vitro* (11). In this communication, we show that FMDV 3D^{pol} also forms fibrils *in vitro*, but only when all of the components necessary for an active elongation assay are present. Furthermore, these structures do not form in the presence of a previously characterized RNA aptamer inhibitory to 3D^{pol} (5).

Both serotype O and C enzymes were used in this study, together with catalytically inactive D388A serotype C mutant protein (a gift from Esteban Domingo, Madrid [1]). Serotype C 3D^{pol} [3D^{pol}(C)] was purified as described previously (7). The 3D^{pol} (serotype O) gene was subcloned from pUb-3Dpol (15) into pET22b-3D^{pol}. The protein was expressed in *Escherichia coli* as a C-terminal hexahistidine fusion and was affinity purified by adsorption to a nickel-Sepharose column (in 50 mM phosphate [pH 7.8], 300 mM NaCl, and elution with a gradient of up to 500 mM imidazole). The 3D^{pol} samples were more than 95% pure, as shown in Fig. 1A. The wild-type (WT) proteins were shown to be active in elongation assays in which [^{32}P]UTP incorporation was measured using a poly(A) template and an oligo(U)$_{15}$ primer (5). However, under these conditions the relationship between enzyme concentration and nucleotide incorporation was not linear, indicative of a degree of cooperativity (Fig. 1B). This is particularly evident with the less-active serotype O enzyme. The addition of $ZnCl_2$ (60 μM) to enhance the activity according to previously reported PV protocols (2, 8, 9, 12, 21) had little effect. Using a similar assay, we showed that the D388A mutant was unable to incorporate [^{32}P]UTP, as expected (Fig. 1C). Interestingly, cooperativity had been demonstrated previously for other viral polymerases, including PV 3D^{pol} (11, 17).

Previously, we selected RNA aptamers to 3D^{pol} of the serotype C virus. RNA aptamers are derived from the process of *in vitro* selection and bind to their target molecules with high affinity and specificity, making them useful as molecular tools and potentially as inhibitors (5). We characterized aptamers that inhibited the

Received 15 July 2011 **Accepted** 18 November 2011

Published ahead of print 7 December 2011

Address correspondence to Nicola J. Stonehouse, n.j.stonehouse@leeds.ac.uk.

M. Bentham and K. Holmes contributed equally to this article.

doi:10.1128/JVI.05696-11

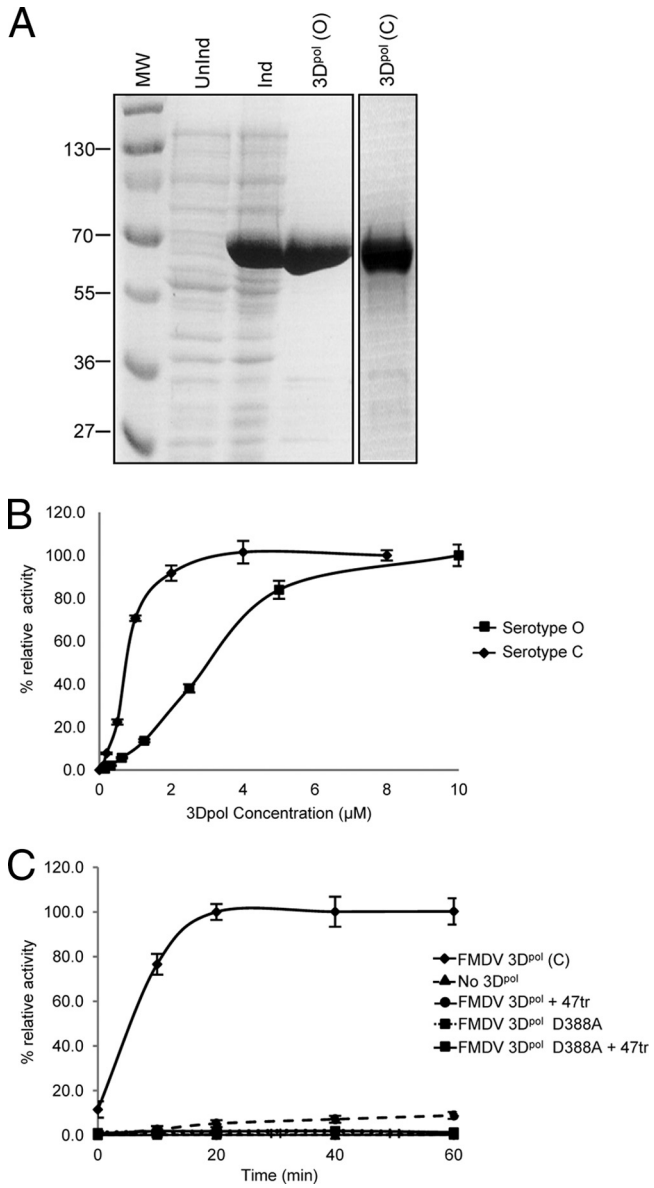

FIG 1 Purification and activity of FMDV 3D^{pol}. (A) Samples of BL21(DE3) pLysS *E. coli* transformed with pET22-3D^{pol}(O) were analyzed by 15% SDS-PAGE either prior to IPTG (isopropyl-β-D-thiogalactopyranoside) induction (UnInd) or 2 h postinduction (Ind). A sample of 3D^{pol}(C) is also shown. MW, molecular weights in thousands. (B) Samples of 3D^{pol}(C) and 3D^{pol}(O) were assayed for elongation activity using the incorporation of [^{32}P]UTP in a MOPS (morpholinepropanesulfonic acid)/NaCl buffer (with 5 mM $MgCl_2$) with a poly(A) template (0.1 μg/μl) and an oligo(U)$_{15}$ primer (1 μM) as described previously (5). Samples were assayed after 20 or 25 min, respectively. (C) The activities of wild-type 3D^{pol}(C) and the active-site mutant D388A (1 μM) were investigated over time in a similar assay. The effects of preincubation with aptamer 47tr (4 μM; 20 min) are also shown.

activity of 3D^{pol} in an elongation assay. One of the aptamers was truncated to 32 mer (F47tr, 5′-GGGUUAACAGAAAACCUCAG UUGCUGGGUUGU-3′), maintaining both its inhibitory capacity and its affinity for 3D^{pol}. Here, we also show that preincubation of 3D^{pol} with 47tr resulted in no incorporation of [^{32}P]UTP (Fig. 1C).

To investigate the products of elongation assays (as described in Fig. 1C), samples were negatively stained prior to examination by transmission electron microscopy (TEM) according to a previously described protocol (22). PV 3D^{pol} was included as a control and shown to form fibrils similar to those described previously (11, 23) (Fig. 2A). In contrast, FMDV 3D^{pol} alone was disordered and aggregated, showing no evidence of defined higher-order structures (Fig. 2C). This result is in agreement with crystallographic data in which differences in crystal packing between the PV and FMDV enzymes suggest that FMDV 3D^{pol} alone is unlikely to form higher-order structures (7). Products of the FMDV elongation assay, however, appeared as ordered fibrils by TEM (Fig. 2B). The fibrils were 250 $\pm$ 27 Å (n = 30) in width and were narrower and more regular than the fibrils observed with isolated PV 3D^{pol} (460 $\pm$ 32Å; n = 30). Fibrils formed by both PV 3D^{pol} and FMDV 3D^{pol} were variable in length. Both C and O 3D^{pol} were capable of fibril formation (Fig. 2B and D, respectively); however, the fibrils formed with the more active serotype C enzyme were more regular in morphology. There was no evidence for the formation of defined higher-order structures other than fibrils, unlike PV 3D^{pol}, which also formed sheets and tubes. Also in contrast with PV 3D^{pol}, all components of an elongation assay were necessary for the formation of the FMDV 3D^{pol} structures (i.e., primer, template, magnesium ions, and NTPs). The presence of dithiothreitol (DTT) or Zn^{2+} had no effect; however, EDTA inhibited both [α-^{32}P]UTP incorporation in the elongation assay and the formation of fibrils as seen by TEM (Table 1), indicating that fibril formation was not a spontaneous event, but rather requires active elongation to occur.

The TEM data correlated with light-scattering measurements of the assay undertaken over the same time scale (Fig. 3). A rapid increase in absorbance at 350 nm was observed with samples of isolated PV 3D^{pol}. A similar, but slower, increase was seen with FMDV 3D^{pol} (saturating after 25 to 30 min) when all components of an elongation assay were present. No increase in light scattering was detected when FMDV 3D^{pol} alone was incubated over time. In addition, substitution of WT 3D^{pol} for the D388A mutant also resulted in no increase in light scattering over time and no fibril formation visible by TEM (Fig. 3 and Table 1). Furthermore, fibrils were not observed in samples treated with RNase A (0.5 μg per 20-μl reaction mixture) or proteinase K (10 μg per 20-μl reaction mixture) at the endpoint of the assay (i.e., after 30 min) (Table 1). This indicates that the fibrils are composed of both 3D^{pol} and single-stranded RNA, rather than an RNA duplex. The walls of the fibrils were measured to be 60 to 70 Å in thickness, consistent with the presence of a single polymerase molecule (7) and suggestive of the structures being tubular in nature. However, further structural studies will be required to confirm this hypothesis. Interestingly, fibrils were also observed when part of the 5′ UTR (negative sense) was used as a template in an elongation assay, although these were less uniform, probably due to the heterogeneity of the RNA used (16). However, this does indicate that the fibrils are not an artifact resulting from the use of a poly(A) template and that 3D^{pol} is able to unfold structured RNA in order to produce a product.

In order to determine the effects of aptamer 47tr on fibril formation, this molecule was included in the assays. Preincubation of 3D^{pol}(C) with 47tr (at an equimolar concentration for 30 min prior to the addition of other components of the elongation assay) inhibited the formation of fibrils observable by TEM (Fig. 2E). This result correlated with no increase in light scattering detect-

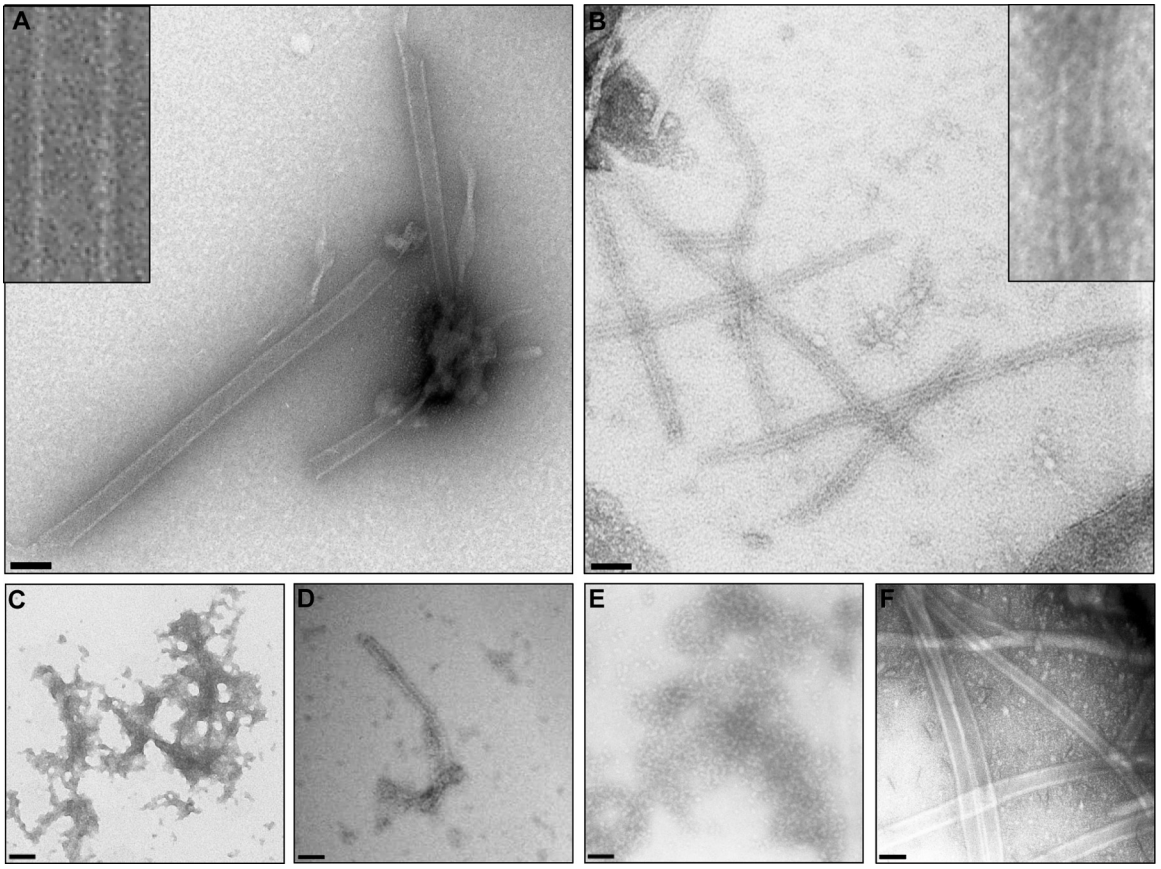

FIG 2 Formation of fibrils during the polymerase elongation assay. (A) PV 3D^{Pol} alone (3 μM). (B) FMDV 3D^{Pol}(C) (1 μM) in the context of a full elongation assay after 30 min. The FMDV fibrils have a regular width averaging 250 Å but exhibit considerable variations in length. (C) FMDV 3D^{Pol}(C) alone. (D) Same as panel B but with the substitution of 3D^{Pol}(O) for 3D^{Pol}(C). (E) Same as panel B but with the addition of equimolar aptamer 47tr. (F) Same as panel A but with the addition of equimolar aptamer 47tr. The insets in panels A and B are higher-magnification views. Negative-stain TEM; scale bars, 500 Å.

able over time in the presence of the aptamer (Fig. 3). However, addition of the aptamer at the endpoint of the assay had no effect. The inhibitory effect of the aptamer on enzyme activity therefore correlates with the absence of fibrils, again demonstrating that these formed only when the polymerase was active. We had demonstrated previously that the aptamer had no inhibitory effect on the ability of PV 3D^{Pol} to incorporate [^{32}P]UTP in an elongation assay (5). In agreement with this, the aptamer had no effect on the formation of PV 3Dpol fibrils by TEM (Fig. 2F).

The formation of a fibrillar replication lattice could have several benefits in viral replication. It could serve to increase the local

TABLE 1 Formation of 3D^{Pol}(C) fibrils under different experimental conditions

Assay or component	Presence of fibrils
Full elongation assay	+
Full elongation assay	
With catalytically inactive 3D^{Pol}	−
Without 3D^{Pol}	−
Without template	−
Without primer	−
With aptamer 47tr (1–5 μM)	−
With RNase (25 μg/ml)	−
With proteinase K (500 μg/ml)	−
With EDTA (10 mM)	−
With DTT (5 mM)	+

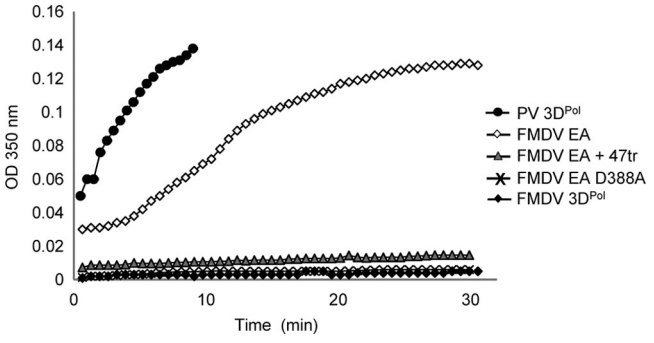

FIG 3 Light-scattering measurements of fibril formation over a time course of up to 30 min at room temperature. Symbols: solid circles, PV 3D^{Pol} alone (3 μM); open diamonds, FMDV 3D^{Pol} elongation assay (EA) with 3 μM 3D^{Pol}(C) and the method described for Fig. 1C; solid diamonds, FMDV 3D^{Pol} alone; shaded triangles, FMDV 3D^{Pol} EA (as above) in the presence of equimolar aptamer 47tr; cross, EA using FMDV 3D^{Pol} active-site mutant D388A. OD_{350} nm, optical density at 350 nanometers.

concentration of components, and a clustering of binding sites could increase the efficiency of replication. It is also tempting to speculate that the higher-order structures have a role in preventing the formation of double-stranded RNA. During replication, a negative-stranded cRNA is first produced, which then acts as a template for the synthesis of positive strands. If the RNA is "coated" in polymerase molecules during this process, forming fibril-like structures, then the formation of a double-stranded negative/positive RNA complex could be prevented. This would allow replication to proceed without the necessity to melt an RNA duplex, which would be energetically demanding and therefore inefficient. It must be noted that *in vivo*, a number of other viral and host proteins (e.g., RNA helicase [10]) are also involved in replication. Our studies are therefore continuing with the use of an FMDV replicon (14) in order to probe the formation of higher-order structures in cells where all replication components are present.

ACKNOWLEDGMENTS

We thank Armando Arias, Graham Belsham, Ian Goodfellow, and Esteban Domingo for $3D^{pol}$ serotype C and O constructs, samples of PV $3D^{pol}$, and the D388A mutant proteins, respectively.

We gratefully acknowledge financial support from BBSRC.

REFERENCES

1. **Arias A, et al.** 2005. Mutant viral polymerase in the transition of virus to error catastrophe identifies a critical site for RNA binding. J. Mol. Biol. **353**:1021–1032.
2. **Cho MW, Richards OC, Dmitrieva TM, Agol V, Ehrenfeld E.** 1993. RNA duplex unwinding activity of poliovirus RNA-dependent RNA polymerase 3Dpol. J. Virol. **67**:3010–3018.
3. **Clarke BE, et al.** 1987. Potential secondary and tertiary structure in the genomic RNA of foot and mouth disease virus. Nucleic Acids Res. **15**: 7067–7079.
4. **Cook PR.** 1999. The organization of replication and transcription. Science **284**:1790–1795.
5. **Ellingham M, Bunka DHJ, Rowlands DJ, Stonehouse NJ.** 2006. Selection and characterization of RNA aptamers to the RNA-dependent RNA polymerase from foot-and-mouth disease virus. RNA **12**:1970–1979.
6. **Escarmís C, Dopazo J, Dávila M, Palma EL, Domingo E.** 1995. Large deletions in the 5′-untranslated region of foot-and-mouth disease virus of serotype C. Virus Res. **35**:155–167.
7. **Ferrer-Orta, C, et al.** 2004. Structure of foot-and-mouth disease virus RNA-dependent RNA polymerase and its complex with a template-primer RNA. J. Biol. Chem. **279**:47212–47221.
8. **Gohara DW, et al.** 2000. Poliovirus RNA-dependent RNA polymerase (3Dpol): structural, biochemical, and biological analysis of conserved structural motifs A and B. J. Biol. Chem. **275**:25523–25532.
9. **Hobson SD, et al.** 2001. Oligomeric structures of poliovirus polymerase are important for function. EMBO J. **20**:1153–1163.
10. **Lawrence P, Rieder E.** 2009. Identification of RNA helicase A as a new host factor in the replication cycle of foot-and-mouth disease virus. J. Virol. **83**:11356–11366.
11. **Lyle JM, Bullitt E, Bienz K, Kirkegaard K.** 2002. Visualization and functional analysis of RNA-dependent RNA polymerase lattices. Science **296**:2218–22122.
12. **Lyle JM, et al.** 2002. Similar structural basis for membrane localization and protein priming by an RNA-dependent RNA polymerase. J. Biol. Chem. **277**:16324–16331.
13. **Mason PW, Bezborodova SV, Henry TM.** 2002. Identification and characterization of a cis-acting replication element (cre) adjacent to the internal ribosome entry site of foot-and-mouth disease virus. J. Virol. **76**:9686–9694.
14. **McInerney GM, King AM, Ross-Smith N, Belsham GJ.** 2000. Replication-competent foot-and-mouth disease virus RNAs lacking capsid coding sequences. J. Gen. Virol. **81**:1699–1702.
15. **Nayak A, Goodfellow IG, Belsham GJ.** 2005. Factors required for the uridylylation of the foot-and-mouth disease virus 3B1, 3B2, and 3B3 peptides by the RNA-dependent RNA polymerase (3Dpol) in vitro. J. Virol. **79**:7698–7706.
16. **Nayak A, et al.** 2006. Role of RNA structure and RNA binding activity of foot-and-mouth disease virus 3C protein in VPg uridylylation and virus replication. J. Virol. **80**:9865–9875.
17. **Pata JD, Schultz SC, Kirkegaard K.** 1995. Functional oligomerization of poliovirus RNA-dependent RNA polymerase. RNA **1**:466–477.
18. **Pelletier J, Sonenberg N.** 1988. Internal initiation of translation of eukaryotic mRNA directed by a sequence derived from poliovirus RNA. Nature **334**:320–325.
19. **Polatnick J, Wool SH.** 1983. Correlation of surface and internal ultrastructural changes in cells infected with foot-and-mouth disease virus. Can. J. Comp. Med. **47**:440–444.
20. **Rowlands DJ, Harris TJ, Brown F.** 1978. More precise location of the polycytidylic acid tract in foot and mouth disease virus RNA. J. Virol. **26**:335–343.
21. **Semler BL, Hanecak R, Dorner LF, Anderson CW, Wimmer E.** 1983. Poliovirus RNA synthesis in vitro: structural elements and antibody inhibition. Virology **126**:624–635.
22. **Stonehouse NJ, Stockley PG.** 1993. Effects of amino acid substitution on the thermal stability of MS2 capsids lacking genomic RNA. FEBS Lett. **334**:355–359.
23. **Tellez AB, et al.** 2011. Interstitial contacts in an RNA-dependent RNA polymerase lattice. J. Mol. Biol. **412**:737–750.